Spectrochimica Acta Part A 94 (2012) 302–307

Contents lists available at SciVerse ScienceDirect

Spectrochimica Acta Part A: Molecular and Biomolecular Spectroscopy

journal homepage: www.elsevier.com/locate/saa

Synthesis, spectroscopy and thermal study of some nickel(II) complexes containing tridentate Schiff bases and substituted amine ligands, X-ray crystal structure of nickel(II) complex

Ali Hossein Kianfar[a,*], Masomeh Bahramian[b], Hamid Reza Khavasi[c]

[a] Department of Chemistry, Isfahan University of Technology, Isfahan 84156-83111, Iran
[b] Department of Chemistry, Yasouj University, Yasouj, Iran
[c] Department of Chemistry, Shahid Beheshti University, G. C., Evin, Tehran 1983963113, Iran

ARTICLE INFO

Article history:
Received 26 December 2011
Received in revised form 29 February 2012
Accepted 9 March 2012

Keywords:
Schiff base complexes
Nickel complexes
Thermogrvimetry

ABSTRACT

Some new tridentate ONO and ONS Schiff base complexes of [NiL(amine)] (L = Salicylidene2-aminophenol and Salicylidene2-aminothiophenol, amine = benzylamine, morpholine, pyrrolidine and piperidine) were synthesized and characterized by IR, UV–vis, ^{1}H NMR spectroscopy and elemental analysis. The geometry of [NiL^2(bzlan)] determined by X-ray crystallography indicates that the complex has planar structure and has four coordinate in the solid state. The thermogravimmetry (TG) and differential thermoanalysis (DTA) of the synthesized complexes were carried out in the range of 20–700 °C, leading to decomposition of ONO type in two stages and of ONS type in three stages. The ONO and ONS complexes were decomposed to NiO and NiS respectively. Thermal decomposition of the complexes is closely the depends upon nature of the Schiff base ligands and proceeds via first order kinetics.

1. Introduction

Schiff bases have been used as ligands because of their ability to create stable coordination compounds with different oxidation states. Schiff base complexes have centered on the role of such complexes in providing synthetic models for the metal containing sites in metallo-proteins and -enzymes [1–5]. The tridentate Schiff bases and their complexes were reported previously [6–8]. Recently, they were reported as effective corrosion inhibitors for some metals in acidic media [9]. Until now, the structure of some nickel [10–12] and copper [13] complexes containing tridentate Schiff bases and amine were studied and their coordination geometries were identified.

Herein we prepared tridentate Schiff bases by the condensation of salicylaldehyde with 2-aminophenol and 2-aminothiophenol. The [NiL(OH$_2$)] complexes of synthesized ligands were prepared in methanol and treated with different amines to prepare [NiL(amine)] complexes [Fig. 1]. The synthesized complexes were identified by IR, NMR, UV–vis spectroscopy and elemental analysis. The structure of [NiL^2(bzlan)] was determined by X-ray crystallography. The thermogravimetry (TG) and differential thermoanalysis (DTA) of the nickel(II) complexes were carried out in the range of 20–700 °C. The thermal decomposition kinetic parameters were also calculated and discussed using Coats and Redfern method [14].

2. Experimental

2.1. Chemicals and apparatus

All of the chemicals and solvents used were reagent quality and used without further purification. Infrared spectra (KBr discs) were recorded on a FT-IR JASCO-680 spectrophotometer in the 4000–400 cm^{-1}. The elemental analyses were determined on a CHN-O-Heraeus elemental analyzor. UV–vis spectra were recorded on a JASCO V-570 spectrophotometer in the 190–900 nm. The ^{1}H NMR spectra were recorded in CDCl$_3$ on DPX-400 MHz FT-NMR. Thermogravimmetry (TG) and differential thermoanalysis (DTA) were carried out on a PL-1500. The measurements were performed in air atmosphere and the heating rate was kept at 10 °C min^{-1}.

2.2. Synthesis

The tridentate Schiff base ligands, L^1(ONO donor) and L^2(ONS donor) and the NiL(OH$_2$) complexes were prepared according to the literature [15].

The NiL(amine) complexes were synthesized by refluxing methanolic solutions of the NiL(OH$_2$) complexes and amines. The reaction was refluxed for 4 h. The resulting red color solution was filtrated. After 24 h, the resulting pin shape crystals were

* Corresponding author. Tel.: +98 311 3913251; fax: +98 311 3912350.
E-mail addresses: akianfar@cc.iut.ac.ir, asarvestani@yahoo.com (A.H. Kianfar).

1386-1425/$ – see front matter © 2012 Elsevier B.V. All rights reserved.
doi:10.1016/j.saa.2012.03.039

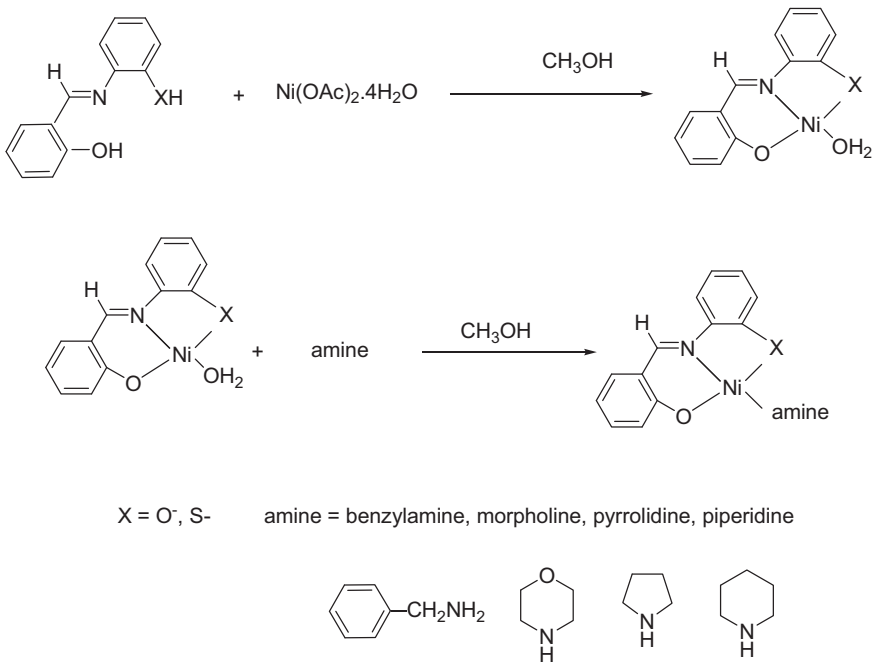

Fig. 1. The structure of nickel complexes.

filtered, washed with methanol and recrystalized from 2:1 ratio of dichloromethane/ethanol and dried in vacuum.

H_2L^1: Yield (90%). ($C_{13}H_{11}NO_2$), FT-IR (KBr cm^{-1}) ν_{max} 3100–2400 (O—H), 1631 (C=N), 1529 (C=C). UV–vis, λ_{max} (nm) (ε, $L\,mol^{-1}\,cm^{-1}$) ($CHCl_3$): 354 (7000), 269 (6000).

H_2L^2: Yield (85%). ($C_{13}H_{11}NOS$), FT-IR (KBr cm^{-1}) ν_{max} 3256 (S—H), 1614 (C=N), 1564 (C=C). UV–vis, λ_{max} (nm) (ε, $L\,mol^{-1}cm^{-1}$) ($CHCl_3$): 345 (6500), 276 (6000).

$NiL^1(H_2O)$: Yield (80%). FT-IR (KBr cm^{-1}) ν_{max} 3424 (O—H), 1616 (C=N), 1539 (C=C). UV–vis, λ_{max} (nm) (ε, $L\,mol^{-1}cm^{-1}$) (Ethanol): 405 (6000), 298 (4700).

$NiL^2(H_2O)$: Yield (80%). FT-IR (KBr cm^{-1}) ν_{max} 3426 (O—H), 1605 (C=N), 1524 (C=C). UV–vis, λ_{max} (nm) (ε, $L\,mol^{-1}cm^{-1}$) (Ethanol): 417 (9000), 272 (15,000).

NiL^1(bzlan): Yield (85%). Anal. calc. for $C_{20}H_{18}N_2O_2Ni$: C, 63.37; H, 4.78; N, 7.39%. Found; C, 62.27; H, 4.57; N, 7.81%. FT-IR (KBr cm^{-1}) ν_{max} 3295, 3186 (N—H), 1605 (C=N), 1530 (C=C). UV–vis, λ_{max} (nm) (ε, $L\,mol^{-1}cm^{-1}$) (Ethanol): 419 (16,000), 249 (16,000), δ (400 MHz, $CDCl_3$, Me4Si) 2.3 (s, 2H, NH_2), 4.0 (s, 2H, CH_2), 6.5–7.4 (m, 13H, Aromatic), 7.8 (s, 1H, HC=N).

NiL^2(bzlan): Yield (85%). Anal. calc. for $C_{20}H_{18}N_2OSNi$: C, 60.79; H, 4.59; N, 7.09%. Found; C, 60.02; H, 4.73; N, 7.45%. FT-IR (KBr cm^{-1}) ν_{max} 3291, 3182 (N–H), 1603 (C=N), 1528 (C=C). UV–vis, λ_{max} (nm) (ε, $L\,mol^{-1}cm^{-1}$) (Ethanol): 424 (9000), 274 (76,000), δ (400 MHz, $CDCl_3$, Me4Si) 2.0 (s, 2H, NH_2), 4.0 (s, 2H, CH_2), 6.6–7.4 (m, 13H, Aromatic), 8.3 (s, 1H, HC=N).

NiL^1(prldn): Yield (80%). Anal. calc. for $C_{17}H_{18}N_2O_2Ni$: C, 59.87; H, 5.32; N, 8.21%. Found; C, 60.27; H, 5.04; N, 8.69%. FT-IR (KBr cm^{-1}) ν_{max} 3287 (N—H), 1604 (C=N), 1539 (C=C). UV–vis, λ_{max} (nm) (ε, $L\,mol^{-1}cm^{-1}$) (Ethanol): 420 (22,000), 249 (22,700), δ (400 MHz, $CDCl_3$, Me4Si) 2.1 (s, H, NH), 1.7–3.4 (m, 8H, CH_2), 6.5–7.5 (m, 8H, Aromatic), 8.1 (s, 1H, HC=N).

NiL^2(prldn): Yield (75%). Anal. calc. for $C_{17}H_{18}N_2OSNi$: C, 57.17; H, 5.08; N, 7.84%. Found; C, 56.54; H, 4.80; N, 8.17%. FT-IR (KBr cm^{-1}) ν_{max} 3215 (N—H), 1604 (C=N), 1573 (C=C). UV–vis, λ_{max} (nm) (ε, $L\,mol^{-1}cm^{-1}$) (Ethanol): 426 (12,000), 271 (24,300), δ (400 MHz, $CDCl_3$, Me4Si) 1.8 (s, H, NH), 1.9–3.3 (s, 8H, CH_2), 6.6–7.4 (m, 8H, Aromatic), 8.4 (s, 1H, HC=N).

NiL^1(pprdn): Yield (80%). Anal. calc. for $C_{18}H_{20}N_2O_2Ni$: C, 60.89; H, 5.68; N, 7.89%. Found; C, 60.14; H, 5.84; N, 8.15%. FT-IR (KBr cm^{-1}) ν_{max} 3278 (N—H), 1602 (C=N), 1527 (C=C). UV–vis, λ_{max} (nm) (ε, $L\,mol^{-1}cm^{-1}$) (Ethanol): 419 (16,000), 249 (9000), δ (400 MHz, $CDCl_3$, Me4Si) 2.8 (s, H, NH), 1.6–3.7 (m, 10, CH_2), 6.5–7.5 (m, 8H, Aromatic), 8.1 (s, 1H, HC=N).

NiL^2(pprdn): Yield (80%). Anal. calc. for $C_{18}H_{20}N_2OSNi$: C, 58.25; H, 5.43; N, 7.54%. Found; C, 58.01; H, 5.56; N, 7.88%. FT-IR (KBr cm^{-1}) ν_{max} 3226 (N—H), 1606 (C=N), 1572 (C=C). UV–vis, λ_{max} (nm) (ε, $L\,mol^{-1}cm^{-1}$) (Ethanol): 425 (8800), 272 (22,000), δ (400 MHz, $CDCl_3$, Me4Si) 1.7 (s, H, NH), 1.4–3.6 (m, 10H, CH_2), 6.6–7.4 (m, 8H, Aromatic), 8.4 (s, 1H, HC=N).

NiL^1(mrpln): Yield (80%). Anal. calc. for $C_{17}H_{18}N_2O_3Ni$: C, 56.87; H, 5.05; N, 7.80%. Found; C, 56.33; H, 5.29; N, 8.08%. FT-IR (KBr cm^{-1}) ν_{max} 3250 (N—H), 1603(C=N), 1528 (C=C). UV–vis, λ_{max} (nm) (ε, $L\,mol^{-1}cm^{-1}$) (Ethanol): 419 (13,000), 249 (3600), δ (400 MHz, $CDCl_3$, Me4Si) 2.1 (s, H, NH), 3.2–3.9 (s, 8H, CH_2), 6.5–7.5 (m, 8H, Aromatic), 8.1 (s, 1H, HC=N).

NiL^2(mrpln): Yield (80%). Anal. calc. for $C_{17}H_{18}N_2O_2SNi$: C, 54.43; H, 4.83; N, 7.46%. Found; C, 53.95; H, 4.72; N, 7.93%. FT-IR (KBr cm^{-1}) ν_{max} 3263 (N—H), 1603(C=N), 1525 (C=C). UV–vis, λ_{max} (nm) (ε, $L\,mol^{-1}cm^{-1}$) (Ethanol): 424 (8000), 272 (22,000), δ (400 MHz, $CDCl_3$, Me4Si) 1.8 (s, H, NH), 1.6–3.3 (s, 8H, CH_2), 6.6–7.4 (m, 8H, Aromatic), 8.4 (s, 1H, HC=N).

2.3. Crystal data collection and processing of [NiL(bzlan)] (*1*)

The X-ray diffraction measurements were made on a STOE IPDS-2T diffractometer with graphite monochromated Mo-K_α radiation. For this complex a yellow plate crystal with a dimension of 0.50 mm × 0.15 mm × 0.20 mm was chosen and mounted on a glass fiber and used for data collection. Cell constants and an orientation matrix for data collection were obtained by least-squares refinement of diffraction data from 4497 unique reflections. Data were collected at a temperature of 298(2) K to a maximum 2θ value of 58.4° in a series of ω scans in 1° oscillations and integrated using the Stoe X-AREA [16] software package. The numerical

absorption coefficient, μ, for Mo-K_α radiation is 1.298 mm^{-1}. A numerical absorption correction was applied using X-RED [17] and X-SHAPE [18] softwares. The data were corrected for Lorentz and Polarizing effects. The structures were solved by direct methods [19] and subsequent difference Fourier maps and then refined on F^2 by a full-matrix least-squares procedure using anisotropic displacement parameters [20]. H atoms were positioned geometrically and constrained to ride on their parent atoms. The NH_2 hydrogen atoms were located in a difference Fourier map and then refined isotropically. Atomic factors are from International Tables for X-ray Crystallography [21]. All refinements were performed using the X-STEP32 crystallographic software package [22].

3. Results and discussion

3.1. IR characteristics

The IR spectra of the nickel(II) Schiff base complexes synthesized here are given in Section 2.2. The phenolic OH stretching frequency of the ligands was approved in the 3100–2500 cm^{-1} region due to the internal hydrogen bonding vibration (O—H···N). This band disappeared in the spectra of the complexes [23–25].

The C=N bond stretching frequency of L^1 and L^2 were approved in 1631 cm^{-1} and 1614 cm^{-1} region respectively [26,27]. In the complexes the C=N stretching shifted to a lower frequencies and observed in 1616–1602 cm^{-1} region, indicating a decrease in the C=N bond order due to the coordinate bond formation between the metal and the imine nitrogen lone pair [26,27].

The amine bands, ν (NH), of [NiL(amine)] complexes were appeared at about 3295–3113 cm^{-1}.

3.2. Electronic spectra

The spectral data of the synthesized complexes are given in Section 2.2. The electronic spectra of the Schiff bases consists of relatively intense bands in the 250–350 nm region, involving $\pi \rightarrow \pi^*$ transition [23,24]. The bands at higher energies correspond to $\pi \rightarrow \pi^*$ transitions of aromatic rings, while the band at lower energies is attributed to the $\pi \rightarrow \pi^*$ transition of azomethine group. Some of the nickel complexes exhibit d–d transition, which overlaps with the azomethine transition.

3.3. ^{1}H NMR spectra

The ^{1}H NMR spectral data for [NiL(amine)] complexes are given in Section 2.2. The CH_2 and NH signals of amines appear in the range of 1.4–4.0 and 1.7–2.8 ppm, respectively. The appearance of the amine signals indicates the coordination of amine ligands in the equatorial position. The signals of aromatic protons lie between 6.5 and 7.5 ppm. The azomethine hydrogen (HC=N) of [NiL(amine)] complexes appears in the range of 7.8–8.4 ppm. In the ONO complexes the HC=N and the NH protons are shifted up field and down field, respectively, while ONS complexes show a reverse trend. The down field chemical shift of the amine NH resonance in the ONO complexes relative to ONS complexes indicates that the N···H···O intramolcular hydrogen bonding is probably strong enough in solution [28].

3.4. Description of the molecular structure of [NiL^2(bzlan)] (**1**)

The complex [NiL^2(bzlan)] was characterized by X-ray diffraction, and the ORTEP representation is shown in Fig. 2. Relevant X-ray diffraction data and selected bond lengths and angles are listed in Tables 1 and 2, respectively. This complex crystallizes in the triclinic space group Pī. The crystal structure of [NiL^2(bzlan)] shows

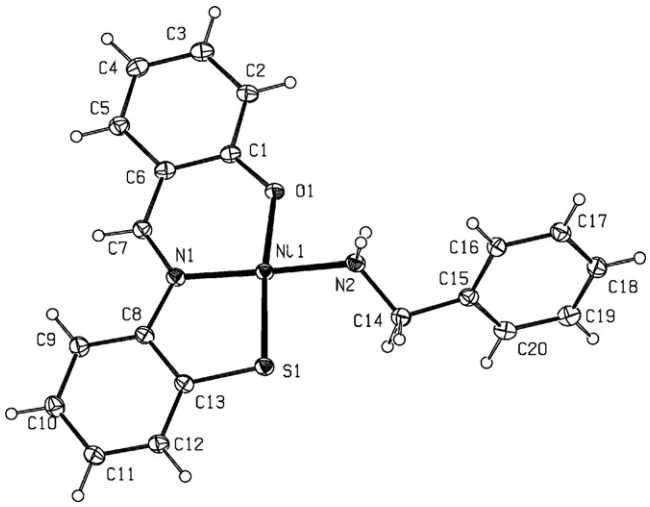

Fig. 2. Crystal structure of [Ni(ONS)(bzlan)] complex.

Table 1
Crystallographic and structure refinements data for complex [Ni(ONS)(bzlan)].

Formula	$C_{20}H_{18}N_2NiOS$
Formula weight	393.12
Temperature/K	298(2)
Wavelength λ/Å	0.71073
Crystal system	Triclinic
Space GROUP	$P\bar{1}$
Crystal size/mm^3	0.50 × 0.20 × 0.15
a/Å	5.6249(6)
b/Å	11.3415(12)
c/Å	14.0736(14)
α/°	69.417(8)
β/°	89.559(8)
γ/°	83.506(8)
Volume/Å^3	834.62(16)
Z	2
Density (calc.)/g cm^{-1}	1.564
θ ranges for data collection	1.5–29.2
F(0 0 0)	298
Absorption coefficient	1.298
Index ranges	$-7 \le h \le 7$ $-14 \le k \le 15$ $-19 \le l \le 19$
Data collected	9437
Unique data (R_{int})	4497, (0.083)
Parameters, restrains	234, 0
Final R_1, wR_2[a] (Obs. data)	0.0578, 0.1532
Final R_1, wR_2[a] (All data)	0.0700, 0.1669
Goodness of fit on F^2 (S)	0.90
Largest diff peak and hole/e Å^3	0.97, −0.71

[a] $R_1 = \Sigma||F_o| - |F_c||/\Sigma|F_o|$, $wR_2 = [\Sigma(w(F_o^2 - F_c^2)^2)/\Sigma w(F_o^2)^2]^{1/2}$.

Table 2
Selected bond distances (Å) and bond angles (°) for [Ni(ONS)(bzlan)].

Bond distances		Bond angles	
Ni1—O1	1.865(2)	O1—Ni1—N1	96.61(11)
Ni1—N1	1.882(2)	N1—Ni1—S1	89.48(9)
Ni1—S1	2.157(1)	S1—Ni1—N2	91.90(10)
Ni1—N2	1.944(3)	N2—Ni1—O1	82.11(12)
O1—C1	1.301(4)	N1—Ni1—N2	177.75(12)
N1—C7	1.318(4)	O1—Ni1—S1	173.15(8)
N1—C8	1.427(4)	Ni1—N2—C14	123.8(2)
S1—C13	1.746(3)	N2—C14—C15	113.3(3)
C6—C7	1.417(5)	C8—N1—C7—C6	−174.7(3)
N2—C14	1.485(4)	N2—C14—C15—C16	47.9(4)
C14—C15	1.508(4)		

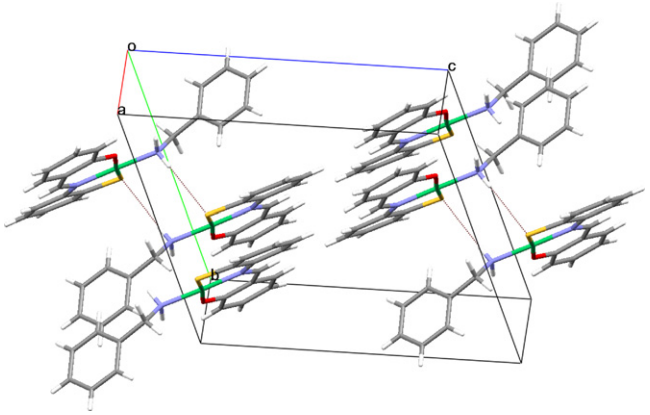

Fig. 3. Crystal packing diagram of [Ni(ONS)(bzlan)].

a tridentate ONS coordination of the Schiff base and a monodentate benzylamine ligand. The angles O(1)—Ni(1)—N(1) = 96.61(11)°, N(1)—Ni(1)—S(1) = 89.48(9)°, S(1)—Ni(1)—N(2) = 91.90(10)° and N(2)—Ni(1)—O(1) = 82.11(12)° indicate that the coordination geometry of the nickel atom is distorted square planar. The Ni ion is 0.13 Å out of the best plane going through the atoms O1, N1, S1 and N2. The Ni—O, Ni—N and Ni—S distances of 1.865(2) Å, 1.882(2) Å and 2.157(2) Å for Ni(1)—O(1), Ni(1)—N(1) and Ni(1)—S(1) respectively are in the ranges observed for analogous compounds of Ni square planar complexes containing ONS Schiff base ligand [10–12]. The Ni—N_{amine} distance (1.944(3) Å) is longer than the Ni—N_{ONS} distance (1.882(2) Å). This is similar to what was observed for [Ni(ONS)(amine)] complexes in which the Ni—N_{amine} distances range from 1.950 Å to 1.957 Å and the Ni—N_{OSN} distances range from 1.873 Å to 1.890 Å [10–12]. The structural data on known nickel (II) square planar complexes having NOS coordination and different monodentate aliphatic N-donor ligands were reported previously [26–28]. The coordination geometries in these complexes are distorted square planar.

As can be seen from the packing diagram of complex **1** (Fig. 3), head-to-tail N(amine)-H···S hydrogen bonds [H2C···$S1^{i}$ = 2.71(6), N2···$S1^{i}$ = 3.527(3) Å and N2-H2C···$S1^{i}$ = 162(5)°, symmetry code(i) $1-x$, $1-y$, $2-z$] between adjacent molecules produce a dimer. It seems that the weak intermolecular $\pi\cdots\pi$ interactions [3.6537(19) Å, symmetry code(ii) $1+x, y, z$] between six-membered phenyl ring and five-membered Ni–S–C–C–N ring are effective in the stabilization of the lattice.

3.5. Thermal analysis

The thermal decomposition of the [NiL(OH_2)] and [NiL(amine)] complexes presented characteristic pathways, depending on the nature of the Schiff base ligands and amines, as can be seen from the TG/DTA curves in Fig. 4. The absence of weight loss up to 80 °C indicates that there is no water molecule in the crystallin solid. Also, in [NiL(OH_2)] complexes, the TG showed weight loss up to 100 °C indicating the presence of water molecule coordinated to complexes [23,29]. All the L^1(=ONO) and L^2(=ONS) complexes were decomposed in two and three steps respectively (Figs. 4–6). The temperature range and the percentage of loss weight for steps were collected in Tables 3–4. Thermalgravimmetry clearly reveals that all the L^1(ONO) complexes obtained here, provide NiO as the final species [25], whereas the L^2(ONS) complexes provide NiS at final stage.

The complex, [NiL^1(OH_2)] decomposes in two steps. The first step occurred up to about 142 °C and was attributed to the release of water. The second mass loss between 410 and 473 °C was assigned to the Schiff base ligand, with the formation of the NiO.

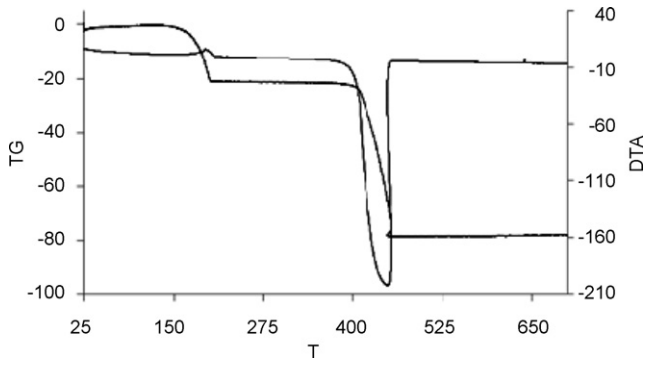

Fig. 4. The TG and DTA of NiL^1(prldn) complex.

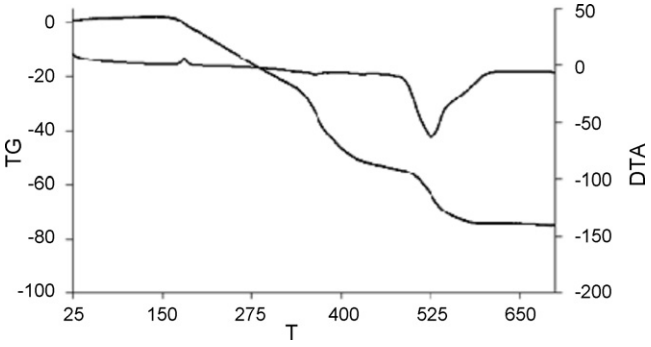

Fig. 5. The TG and DTA of NiL^2(bzlan) complex.

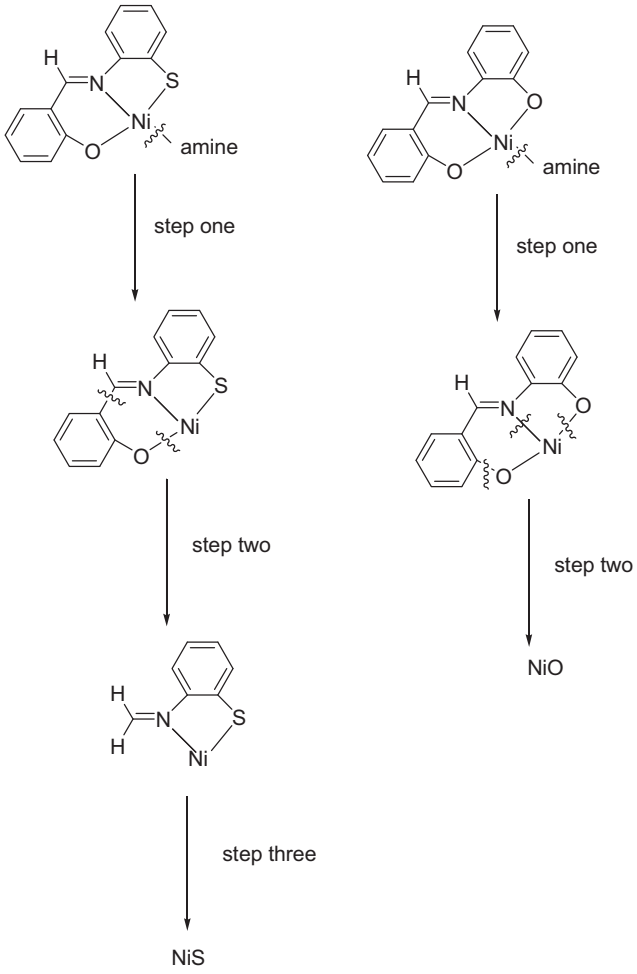

Fig. 6. The proposed decomposition pathway of the nickel complexes.

Table 3
Thermal and kinetics parameters for nickel complexes.

Compounds	ΔT (°C)[a]	Percent (%)[b]	E^* (kJ mol^{-1})	A^* (s^{-1})	S^* (kJ mol^{-1} K^{-1})	H^* (kJ mol^{-1})	G^* (kJ mol^{-1})
NiL^1(H$_2$O)	202–258	5(6)	26.8	2.5×10^{-1}	−250	24.8	86
	410–473	66(67)	396.9	7.5×10^{26}	266	393.2	273
NiL^1(prldn)	150–211	20(21)	148.9	3.6×10^{14}	37	147.3	140
	400–465	58(57)	141.2	6.8×10^{7}	−98	137.4	180
NiL^1(mrpln)	163–221	20(24)	169.9	1.5×10^{16}	68	168.2	154
	393–487	52(54)	165.2	5.5×10^{9}	−61.7	161.6	189
NiL^1(pprdn)	124–205	20(24)	184.3	5.9×10^{18}	118	182.7	159
	400–474	55(55)	212.2	1.8×10^{13}	5.5	208.5	206
NiL^1(bzlan)	174–214	25(28)	284.9	3.5×10^{29}	320	283.3	220
	414–474	51(48)	202	3.4×10^{12}	−8.3	198.4	202

[a] The temperature range of decomposition pathways.
[b] Precent of weight lose found (calculated).

Table 4
Thermal and kinetics parameters for nickel complexes.

Compounds	ΔT (°C)[a]	Percent (%)[b]	E^* (kJ mol^{-1})	A^* (s^{-1})	S^* (kJ mol^{-1} K^{-1})	H^* (kJ mol^{-1})	G^* (kJ mol^{-1})
NiL^2(H$_2$O)	167–197	5(6)	175.03	3.9×10^{12}	9.4×10^{-2}	173.5	1.7×10^{2}
	332–432	31(31)	127.76	1.9×10^{9}	-6.9×10^{1}	124.7	1.5×10^{2}
	502–586	33(33)	106.25	1.6×10^{6}	-1.3×10^{2}	101.8	1.7×10^{2}
NiL^2(prldn)	175–315	22(20)	39.8	7.9	−225	38.1	85
	354–447	29(26)	58.2	89.9	−211	54.6	147
	500–567	24(28)	84.7	1.1×10^{3}	−190	80.2	184
NiL^2(pprdn)	187–334	22(23)	44.3	15.8	−219	42.4	90.5
	362–493	29(25)	24.7	0.1	−267	21.1	137
	481–555	21(27)	70.8	1.5×10^{4}	−169	66.5	153
NiL^2(bzlan)	178–348	27(27)	30.2	0.6	−245	28.7	73.6
	351–406	25(24)	81.7	1.1×10^{4}	−169	78.8	139
	500–604	22(25)	91.2	2.5×10^{3}	−185	86.8	185
NiL^2(mrpln)	180–330	24(23)	50.2	7.7×10^{1}	-2.1×10^{2}	48.6	8.9×10^{1}
	350–440	26(25)	65.31	2.4×10^{4}	-1.6×10^{2}	62.2	1.2×10^{2}
	450–570	24(27)	40.9	8.4×10^{-1}	-2.5×10^{2}	36.5	1.7×10^{2}

[a] The temperature range of decomposition pathways.
[b] Precent of weight lose found (calculated).

The complexes, [NiL^1(amine)] decompose in two steps. The first step occurred in the range 124–229 °C and was attributed to the release of amine. The second mass loss between 393 and 487 °C was assigned to the Schiff base ligand, with the formation of the NiO.

The complex, [NiL^2(OH$_2$)] decomposes in three steps. The first step occurred up to about 167 °C and was attributed to the release of water. The second thermal event that observes between 332 and 432 °C is related to release of phenoxy. The third mass loss between 502 and 586 °C was assigned to the rest of the ligand, with the formation of the NiS.

The complexes, [NiL^2(amine)] decomposes in three steps. The first step occurs in the range of 175–348 °C and was attributed to the release of amine. The phenoxy moiety of the Schiff base ligand is released in the second thermal event between 350 and 493 °C. The thrid mass loss between 450 and 604 °C was assigned to the rest of the ligand, with the formation of the NiS.

3.6. Kinetics aspects

All the well-defined stages were selected to study the kinetics of decomposition of the complexes. The kinetics parameters (the activation energy E and the pre-exponential factor A) were calculated using the Coats–Redfem equation [14],

$$\log\left[\frac{g(\alpha)}{T^2}\right] = \log\frac{AR}{\phi E}\left[1-\frac{2RT}{E_a}\right] - \frac{E_a}{2.303\,RT} \quad (1)$$

where $g(\alpha)=[(W_f)/(W_f-W)]$. In the present case, a plot of L.H.S (left hand side) of this equation against $1/T$ gives straight line (Fig. 7) whose slope and intercept are used to calculate the kinetics parameters by the least square method. The goodness of fit was checked by calculating the correlation coefficient. The other systems and their steps show the same trend.

The entropy of activation $S^{\neq}$ was calculated using the equation

$$A = \frac{kT_s}{h}e^{S^{\#}/R} \quad (2)$$

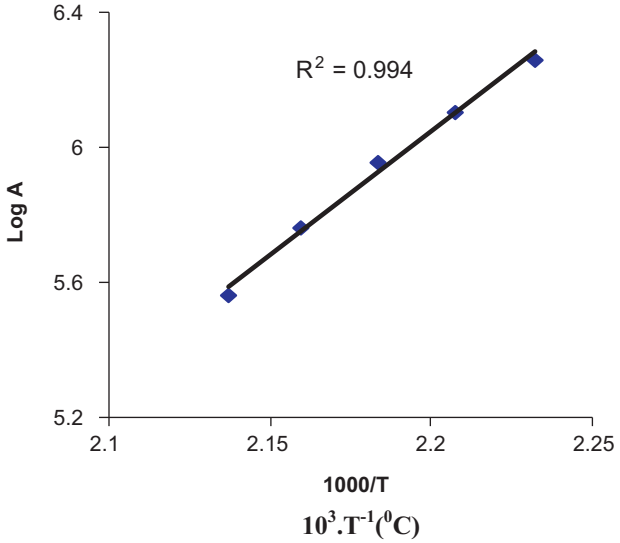

Fig. 7. Coats–Redfern plots of NiL^1(prldn) complex, step 1, $A=\frac{\log(W_f)/(W_f-W)}{T^2}$.

where k, h and T_s are the Boltsman constant, the Planck's constant and the peak temperature respectively. The enthalpy and free energy of activation were calculated using equations

$$G^{\#} = H^{\#} - TS^{\#} \quad (3)$$

$$E_a = H^{\#} + RT \quad (4)$$

The various kinetic parameters calculated are given in Tables 3–4. The activation energy (E_a) in the different stages are in the range 19.81–154.56 kJ mol^{-1}. The respective values of the pre-exponential factor (A) vary from 1.41×10^2 to 4.45×10^{12} s^{-1}. The corresponding values of the entropy of activation ($S^{\neq}$) are in the range of $^{-}$338 to -35 J mol^{-1}. The corresponding values of the enthalpy of activation ($H^{\neq}$) are in the range of 19.05–149.40 kJ mol^{-1}. The corresponding values of the free energy of activation ($G^{\neq}$) are in the range of 158.76–209.45 kJ mol^{-1}. There is no definite trend in the values of the activation parameters among the different stages in the present series.

4. Conclusions

Considering the spectral, structural and thermogravimmetrical properties of nickel(II) tridentate Schiff base complexes the following conclusions have been made.

1. The [NiL (amine)] complexes are relatively planar.
2. Coordinated water was confirmed by thermalgravimmetry of [NiL(OH_2)] complexes.
3. Coordinated amines were confirmed by spectroscopy, thermalgravimmetry and X-ray crystallography.
4. The complexes containing ONO ligand decomposed in two steps while ONS complexes decomposed in three steps.
5. The ONO complexes decomposed to NiO while the ONS complexes decomposed to NiS.

Appendix A. Supplementary data

Supplementary data associated with this article can be found, in the online version, at doi:10.1016/j.saa.2012.03.039.

References

[1] P.K. Mascharak, Coord. Chem. Rev. 225 (2002) 201–214.
[2] J.G. Muller, L.A. Kayser, S.J. Paikoff, V. Duarte, N. Tang, R.J. Perez, S.E. Rokita, C.J. Burrows, Coord. Chem. Rev. 185–186 (1999) 761–774.
[3] D.P. Kessissoglou, Coord. Chem. Rev. 185–186 (1999) 837–858.
[4] J.W. Pyrz, A.L. Roe, L.J. Stern, L. Que, J. Am. Chem. Soc. 107 (1985) 614–620.
[5] V.E. Kaasjager, L. Puglisi, E. Bouwman, W.L. Driessen, J. Reedijk, Inorg. Chim. Acta 310 (2000) 183–190.
[6] A.A. Soliman, G.G. Mohamed, Thermochim. Acta 421 (2004) 151–159.
[7] D.M. Boghaei, M. Gharagozlou, Spectrochim. Acta Part A 67 (2007) 944–949.
[8] S. Chattopadhyay, M.S. Ray, S. Chaudhuri, G. Mukhopadhyay, G. Bocelli, A. Ghosh, Inorg. Chim. Acta 359 (2006) 1367–1375.
[9] M. Behpour, S.M. Ghoreishi, N. Soltani, M. Salavati-Niasari, M. Hamadanian, A. Gandomi, Corros. Sci. 50 (2008) 2172–2181.
[10] D. Ulku, M.N. Tahir, G. Ucar, O. Atakol, Acta Crystallogr. Sect. C: Crystallogr. Struct. Commun. 52 (1996) 1884–1885.
[11] Y. Elerman, M. Kabak, I. Svoboda, J. Chem. Crystallogr. 26 (1996) 29–32.
[12] M.N. Tahir, D. Ulku, O. Atakol, A. Kenar, Acta Crystallogr. Sect. C: Crystallogr. Struct. Commun. 52 (1996) 2178–2180.
[13] R.N. Patel, V.L.N. Gundla, D.K. Patel, Polyhedron 27 (2008) 1054–1060.
[14] A.W. Coats, J.P. Redfern, Nature 201 (1964) 68–69.
[15] A.A. Soliman, W. Linert, Thermochim. Acta 338 (1999) 67–75.
[16] Stoe & Cie, X-AREA, Version 1.30: Program for the Acquisition and Analysis of Data, Stoe & Cie GmbH, Darmatadt, Germany, 2005.
[17] Stoe & Cie, X-RED, Version 1.28b: Program for Data Reduction and Absorption Correction, Stoe & Cie GmbH, Darmatadt, Germany, 2005.
[18] Stoe & Cie, X-SHAPE, Version 2.05: Program for Crystal Optimization for Numerical Absorption Correction, Stoe & Cie GmbH, Darmatadt, Germany, 2004.
[19] G.M. Sheldrick, SHELX97. Program for Crystal Structure Solution, University of Göttingen, Germany, 1997.
[20] G.M. Sheldrick, SHELX97. Program for Crystal Structure Refinement, University of Göttingen, Germany, 1997.
[21] International Tables Foe X-ray Crystallography, Vol. C, Kluwer Academic Publisher, Doordrecht, The Netherlands, 1995.
[22] Stoe & Cie, X-STEP32, Version 1.07b: Crystallographic Package, Stoe & Cie GmbH, Darmstadt, Germany, 2000.
[23] B.S. Kumar, D.N. Garg, Spectrochim. Acta Part A 59 (2003) 229–234.
[24] A. Balasubramanian, S. Anthonysamy, Inorg. Chem. Commun. 8 (2005) 908–911.
[25] D.N. Kumar, B.S. Garg, Spectrochim. Acta Part A 59 (2006) 141–147.
[26] A.H. Kianfar, L. Keramat, M. Dostani, M. Shamsipur, M. Roushani, F. Nikpour, Spectrochem. Acta Part A 77 (2010) 424–429.
[27] A.H. Kianfar, V. Sobhani, M. Dostani, M. Samsipur, M. Roushani, Inorg. Chim. Acta 355 (2011) 108–112.
[28] M. Amirnasr, K.J. Schenk, S. Meghdadi, Inorg. Chim. Acta 338 (2002) 19–26.
[29] A.A. Soliman, J. Therm. Anal. Calorim. 63 (2001) 221–231.